different from Eq. (5). The Lu^{3+} ion has a completely filled $4f$ shell, and hence no magnetic hyperfine interaction, so the spin Hamiltonian is

$$\mathcal{H}=P[I_z^2-(\tfrac{1}{3})I(I+1)].$$

This pure quadrupole interaction is characterized by a linear dependence of ϵ upon $1/T$ for small values of ϵ. This is true also for the related quantity $W(90°)-W(0°)$. In Fig. 10 we show the experimental $W(90°)-W(0°)$ versus $1/T$ plot obtained for the 208-keV transition in Hf^{177} [15] using Meyer's T-T^* relation; in Figure 11 the new temperature scale has been used. The improvement in agreement of the temperature dependence with theory is evident and striking, and provides further reason for confidence in the new scale.

[15] J. Blok and D. A. Shirley, Phys. Rev. (to be published).

VI. CONCLUSIONS

This work was undertaken to try to explain several anomalous temperature dependencies observed in nuclear orientation experiments using NES. The new temperature scale has given satisfactory resolution of the anomaly for Ce^{137m} in the region $1/T<40$, and for Lu^{177} in the entire temperature range. This success indicates that the new scale is a definite improvement over that which was previously available, and further demonstrates the value of nuclear orientation as an accurate thermometric technique in the near-millidegree range.

PHYSICAL REVIEW VOLUME 143, NUMBER 1 MARCH 1966

Second-Sound Attenuation Associated with Hot Ions in Liquid He II†

L. Bruschi, B. Maraviglia, and P. Mazzoldi
Istituto di Fisica Università di Roma, Roma, Italy
(Received 3 August 1965)

An extra attenuation of a second-sound wave associated with the motion of hot ions in liquid helium II has been investigated in the range of temperatures 0.87–1.40°K. Such an attenuation manifests itself as a threshold phenomenon at a well-defined electric field E_α, which is found to coincide with the critical field E_C at which a "persistence" of the drift velocity $\langle V_D\rangle$ begins. The existence of a threshold indicates that there is a quite different hydrodynamical regime beyond the threshold. The threshold field has the temperature dependence $E_\alpha=Ae^{-\Delta_S/T}$, with $\Delta_S=7.69\pm0.13$°K. Δ_S varies with pressure analogously to the Δ of rotons measured by neutron diffraction. It is found experimentally that the extra attenuation is an effect strictly associated with the ion. The attenuation is not interpretable in terms of the single-vortex-ring models so far existing. Comparisons are made with analogous experiments where the interaction between second-sound waves and vorticity is investigated.

INTRODUCTION

THE study of the drift velocity $\langle V_D\rangle$ of positive and negative ions in liquid helium II has shown that at sufficiently high electric fields, the drift velocity, after having reached a maximum value, undergoes a sharp decrease (Fig. 1). This phenomenon, investigated in a range of temperatures between 0.87 and 1°K is independent of temperature and the sign of the charge.[1,2]

Such a behavior can be justified by assuming that a vortex ring is coupled with the moving ion. According to this model the dependence of the drift velocity on the electric field E can be represented by

$$\ln(\langle V_D\rangle/E)=A-BE, \quad (1)$$

where A and B are temperature-dependent parameters.

For still higher fields the drift velocity no longer obeys the relation (1) and, after passing through a minimum, increases linearly. The electric field E_M, corresponding to the minimum of the drift velocity, is a function of the density of rotons. This is confirmed by the dependence of E_M upon pressure and temperature.

It has been recently discovered[3] that at a value E_C of electric field close to E_M a "persistence" of the drift velocity begins. Essentially, "persistence" means that an ion beam, after having been in an electric field higher than E_C, can propagate through macroscopic distances in a zero electric field, with only a small loss of its energy. This fact seems to be extraordinary, considering the high roton density existing at the temperatures at which the measurements were made. Indeed, such an effect has been observed at temperatures up to 1.4°K.

In order to study the nature of the "persistence" of the drift velocity, and its possible connection with the

† Work supported in part by the Consiglio Nazionale delle Ricerche and Istituto Nazionale di Fisica Nucleare.

[1] G. Careri, S. Cunsolo, P. Mazzoldi, M. Santini, in *Proceedings of the Ninth International Conference on Low-Temperature Physics, Columbus, Ohio,* edited by J. G. Daunt, D. V. Edwards, F. J. Milford, and M. Yagub (Plenum Press, Inc., New York, 1965).

[2] G. Careri, S. Cunsolo, P. Mazzoldi, and M. Santini (to be published).

[3] P. Mazzoldi and M. Santini (to be published).

previously given explanation for the sharp decrease, we have endeavored to use second-sound waves, which have been shown by others[4,5] to be sensitive to the existence of vorticity. In fact, an extra attenuation of a second sound wave, propagating parallel or transverse to the ionic beam, has been found.[1]

EXPERIMENTAL TECHNIQUE

In order to detect very small extra attenuation coefficients of second sound we have preferred to use a resonance technique rather than a pulse technique.[4] The sensitivity of our resonance technique to second-sound amplitude variations is greater than 0.1%.

A. Cells

A very large number of resonant cavities, built in different geometries, with walls of Plexiglas, lavite, and copper have been used. In Fig. 2 are represented the ones most commonly used. The thermometer and the heater for receiving and generating second-sound waves are at opposite ends of the resonant cavity. The thermometer and the heater are made of a thin layer of carbon deposited on an insulating support. Our thermometers have temperature coefficients of about 30 $k\Omega$/deg and a resistence of about 20 $k\Omega$ at 0.9°K. The heater has a resistance of about 500 Ω at that temperature and is almost temperature-independent in the range of temperatures of our measurements.

1. Cells of Type A

The resonant cavity A is a cylinder where the second-sound wave propagates parallel to the ionic beam. Electric charges of both sign are generated by ionization of helium atoms by a Po^{210} source deposited on a gold-plated grid. By applying an electric field between the source S and the grid A, where $E_{SA} \ll E_M$, an ionic beam of the chosen charge sign and density can be extracted. In our experiments we obtain a maximum density of charge of about 10^6 ions/cm^3. Then the ionic beam passes into the space between the grid A and the collector C where there is a chosen electric field. The distances between the electrodes are varied in a range which lies between 2 and 15 mm, with an error of the order of about 2%; this implies an error of about 3% in our calculation of the electric fields. Once the length of the cavity is fixed, we choose a width as small as possible to minimize the amplitude of the second-sound wave transverse to the ionic beam.

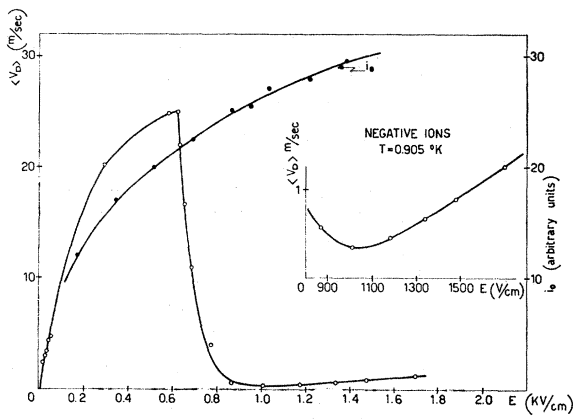

FIG. 1. The drift velocity $\langle V_D \rangle$ of negative ions and a magnification of the minimum at high fields is plotted versus the electric field E. i_0 is the current measured at the ion collector.

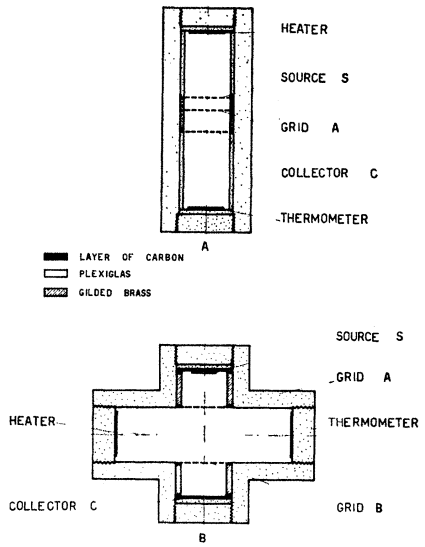

FIG. 2. A schematic view of the cells of types A and B used in our experiments.

2. Cells of Type B

This type of cell consists of two orthogonal cylinders. One contains the polonium source S, two grids A and B, and the collector C; the other is the resonant cavity. Naturally the ratio of the lengths of the orthogonal cavities must be chosen so as to avoid a coincidence of resonance in the two orthogonal cylinders.

3. Pressure Cell

The pressure cell consists of a copper cavity connected to a cylinder containing ^{4}He at a pressure of 100 atm, through a capillary with an inner diameter of 1 mm. The 99% pure He gas from the cylinder is further purified by means of a liquid He trap. The pressure is measured by manometers with an absolute error of 0.2 atm. In the pressure cell an arrangement analogous to Fig. 2(a) has been used.

[4] H. E. Hall and W. F. Vinen, Proc. Roy. Soc. **A238**, 204, 215 (1956).

[5] W. F. Vinen, Proc. Roy. Soc. **A240**, 114, 128 (1957); **A242**, 493 (1957); **A243**, 400 (1957). V. P. Peshkov and V. B. Stryukov, Zh. Eksperim. i Teor. Fiz. **41**, 1443 (1961) [English transl.: Soviet Phys.—JETP **14**, 1031 (1962)].

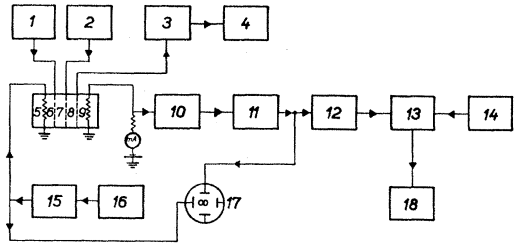

1 HIGH VOLTAGE GENERATOR
2 HIGH VOLTAGE GENERATOR
3 ELECTROMETER
4 CHART RECORDER
5 HEATER
6 POLONIUM SOURCE
7 GRID
8 COLLECTOR
9 THERMOMETER
10 MATCHED PRE-AMPLIFIER
11 NARROW BAND AMPLIFIER
12 RECTIFIER INTEGRATOR
13 DIFFERENTIAL AMPLIFIER
14 REFERENCE VOLTAGE
15 CATHODE FOLLOWER
16 OSCILLATOR
17 SCOPE
18 CHART RECORDER

FIG. 3. Block diagram of the electronic equipment used for the second-sound attenuation measurements.

B. Electronic Equipment

The heater is driven through a cathode follower by a high-stability Wien bridge oscillator. The oscillator was calibrated by a digital counter and its frequency stability was greater than 0.1%. The power dissipated in the heater is kept at a value lower than 10^{-4} W/cm^2 to avoid any irreversible effects. The amplitude of the oscillator signal is controlled by a thermistor

The second-sound wave is detected by a thermometer activated by a current of about 5.10^{-5} A. The received signal, after being amplified by 40 dB, passed through a narrow band amplifier (Fig. 3). The second amplification is 46 dB. Finally the signal, after a rectification and integration, is compared to a reference voltage through a differential amplifier. The chart recorder 18 (Fig. 3) gives a direct measurement of the area of the rectified sinusoidal wave. This area is directly proportional to the sinusoidal wave amplitude.

C. Measuring Technique

The total attenuation coefficient of second sound[4] can be written as

$$\alpha=\alpha_0+\alpha_{\text{ion}},$$

where α_0 is the residual attenuation without ions and α_{ion} is the extra attenuation due to the presence of ions.

The extra attenuation coefficient α_{ion} can be calculated by using the Q of the half-wave resonant cavity. Q is the ratio $\nu/\delta\nu$, where $\delta\nu$ is the width of the resonant curve where the amplitude is $\frac{1}{2}\sqrt{2}$ of the maximum value corresponding to the frequency ν. Once the Q_0 of the cavity is known, it can be shown that:

$$\alpha_{\text{ion}}=(\pi\nu/\mu_2 Q_0)(Q_0/Q-1), \qquad (2)$$

where Q_0/Q can be determined by the ratio of the maximum resonant amplitudes without and with ions present and μ_2 is the second-sound velocity. The validity of substituting the ratio Q_0/Q with the amplitude ratio A_0/A has been verified in our experiments.

If ions occupy only a part x of the whole length y of the resonant cavity, the attenuation coefficient becomes

$$\alpha_{\text{ion}}=\frac{\pi\nu}{\mu_2 Q_0}\left(\frac{A_0}{A}-1\right)\frac{y}{x}=\frac{\pi}{2Q_0}\left(\frac{A_0}{A}-1\right)\frac{1}{x} \qquad (3)$$

when the wave length of second-sound $\lambda=2y$. Although the sensitivity of our method for the detection of second-sound amplitude variations is about 0.1%, the existence of thermal fluctuations in the bath and the noise of the thermometer give rise to a relative error in α_{ion} up to 6%. This arises essentially from the determination of A_0/A.

The drift velocity of ions is measured by a time-of-flight method.[6] This method consists in the determination of the time taken by the ions to travel the distance from the grid A to the collector C [Fig. 2(a)]. The accuracy of the determination of the drift velocity is about 2%.[7]

Temperature is measured using an Allen-Bradley carbon resistor of $\frac{1}{2}$W and is stabilized by an electronic thermoregulator with an accuracy of about 10^{-4}°K. The thermoregulator has been built in this laboratory and is quite similar to the one of Edwards.[8] Ionic currents are of the order of 10^{-12} A and are measured with ECKO vibrating-reed electrometers.

EXPERIMENTAL RESULTS

A. Negative Ions

As already mentioned in the Introduction, a new phenomenon of particular interest begins to be observed at an electric field E_C close to the field E_M. Experimentally one finds that when the electric field between the source S and the grid A [Fig. 2(a)] reaches the value E_C (Fig. 4), a current i_C is collected by the collector with a zero applied electric field between the grid A and the collector. This phenomenon has been called "persistence" of the drift velocity.

We detect the "persistence" of the drift velocity even when the distance d between the grid and the collector is as large as 15 mm. However, the collector current i_C decreases exponentially with the distance d; $i_C=i_0e^{-d/\beta}$. Here β is a distance which can be thought of as a kind of penetration depth for the electric charges. β turns out to be an increasing function of the extracting field E_{SA}.

An extraordinary extra attenuation of a second-sound wave, propagating parallel to the ionic beam, appears at an electric field E_α coinciding with E_C. In Fig. 4 are presented, for the sake of comparison, the minimum of the drift velocity $\langle V_D\rangle$, the collector current i_C, and the variation of the second sound amplitude ΔT (defined as A_0-A) versus the electric field. The coincidence

[6] S. Cunsolo, Nuovo Cimento **21**, 76 (1961).
[7] G. Careri, S. Cunsolo, and P. Mazzoldi, Phys. Rev. **136**, A303, (1964).
[8] O. Edwards, thesis, University of Oxford, 1959 (unpublished).

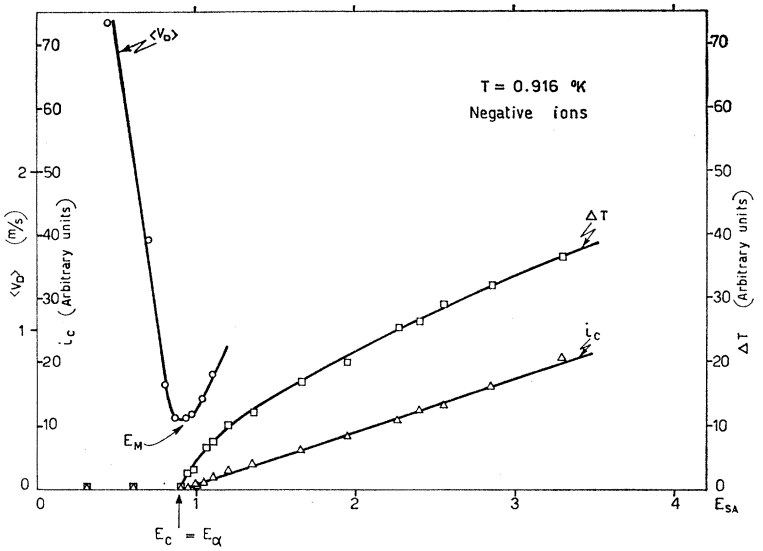

FIG. 4. The critical field for the variation ΔT of the second sound amplitude caused by negative ions is compared to the critical field E_{SA} between the source S and the grid A, when the passage of ions from the grid towards the collector begins and is revealed by a current i_C. The field between the grid A and the collector C is kept at a zero value. It is worth noting that the minimum of the drift velocity $\langle V_D \rangle$ is rather close to the critical field for the second-sound attenuation.

of E_C with E_α is immediately obvious. No substantial difference is noted in the extra attenuation of a second-sound wave propagating perpendicular to the ionic beam.

Moreover, no variation is found in the second-sound attenuation, either when the second-sound propagates in the area with supercritical field ($E > E_C$) or in the area with zero electric field. In other words, this means that if the resonant cavity [Fig. 2(b)] is translated from the interspace between the grid A and grid B to the space between the source S and the grid A, no appreciable difference in the extra attenuation coefficient is observed.

Such measurements are performed with the following electric fields:

$$E_{SA} \gtrless E_C,$$
$$E_{AB} = E_{BC} = 0,$$

where E_{SA} is the electric field between the source S and the grid A, and where E_{AB} and E_{BC} are the fields between the grids A and B and between the grid B and the collector, respectively.

The ratio of the extra attenuation coefficient and the residual attenuation α_{ion}/α_0 is plotted versus the electric field E in Fig. 5 (curve A), whereas curve B represents the same ratio, normalized per unit charge. A direct comparison clearly shows that the slope variation exhibited by the curve A is due only to the variation of the density of charge. The extra attenuation coefficient seems to be linear with respect to the electric field, if one excludes the region close to the critical field E_α. To test the linear dependence of the attenuation coefficient on charge density, we have varied the density of charge ρ up to 25% (ρ being generally about 10^6 ions/cm^3). Actually, in the apparatus A of Fig. 2, keeping a constant supercritical field between the grid A and the collector C and varying the extracting subcritical field be-

TABLE I. Here are listed the ratios of the collector current, the corresponding ratios of the extra attenuation coefficients, and the threshold fields $E_{\alpha 1}$, $E_{\alpha 2}$, $E_{\alpha 3}$ corresponding, respectively, to the three values 400, 200, 100 V/cm of the extracting field.

$\frac{i_{C_1}}{i_{C_2}} = 1.13 \pm 0.02$	$\frac{\alpha_{ion1}}{\alpha_{ion2}} = 1.13 \pm 0.02$	$E_{\alpha_1} = 810 \pm 25$ V/cm
$\frac{i_{C_1}}{i_{C_3}} = 1.10 \pm 0.02$	$\frac{\alpha_{ion2}}{\alpha_{ion3}} = 1.08 \pm 0.02$	$E_{\alpha_2} = 800 \pm 30$ V/cm
$\frac{i_{C_1}}{i_{C_3}} = 1.24 \pm 0.03$	$\frac{\alpha_{ion1}}{\alpha_{ion3}} = 1.25 \pm 0.02$	$E_{\alpha_3} = 800 \pm 15$ V/cm

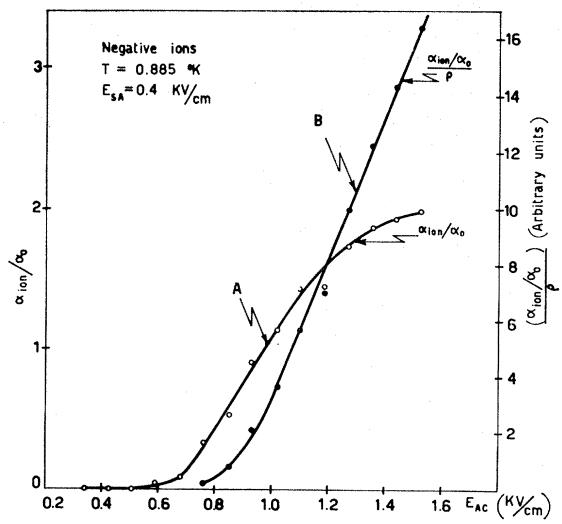

FIG. 5. This figure contains a direct comparison of the plot versus the electric field E of: (a) the extra attenuation coefficient α_{ion} relative to α_0; (b) the ratio of the relative extra attenuation coefficient α_{ion}/α_0 and the charge density ρ.

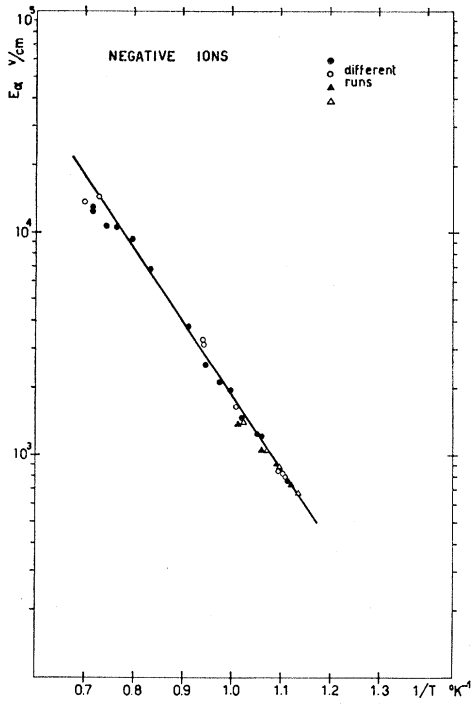

FIG. 6. The threshold field E_α on a logarithmic scale is represented as a function of the reciprocal absolute temperature T^{-1}. The circles and triangles denote experimental points obtained in different runs.

tween the source S and the grid A, it has been noted that the ratios of the currents at the collector coincide with the ratios of the corresponding extra attenuation coefficients. Some of these ratios are shown in Table I. The three extracting fields corresponding to the index 1, 2, and 3 are, respectively, 400, 200, and 100 V/cm. These measurements have been performed for eight values of the electric field E_{AC}, kept greater than E_α. At the same time it has been verified that the electric field E_α is independent of the density of charge (Table I).

The determination of the extra attenuation coefficient at fixed conditions has shown no appreciable variation when working either with the fundamental frequency of second-sound or with higher-order ones. Moreover it has been noted that, when extra attenuation occurs, there is no variation of that frequency, which corresponds to the maximum of resonance. In other words no fictitious variation of the second-sound amplitude is due to a variation of the peak of resonance.

The dependence of E_α upon temperature is represented in Fig. 6, where is plotted E_α versus $1/T$. This dependence can be represented by the exponential relation

$$E_\alpha = Ae^{-\Delta S/T}. \quad (4)$$

The measurements have been extended to a range of temperatures $0.878 < T < 1.426$°K. Using a best-fit-calculation we find

$$A = 4.024\ 10^6\ \text{V/cm},$$
$$\Delta_S = 7.69 \pm 0.13\text{°K}.$$

TABLE II. Comparison of $\Delta_S - (\Delta_S)_P$ with the corresponding values obtained by neutron diffraction and by thermodynamical calculation.

P (atm)	$(\Delta_S - \Delta_{SP})_{\text{EXPER.}}$ (°K)	$(\Delta - \Delta_P)_{\text{NEUTR.}}$ (°K)	$(\Delta - \Delta_P)_{\text{THERM.}}$ (°K)
3.00±0.20	0.235±0.060	0.20±0.02	0.30±0.30
6.25±0.20	0.423±0.045	0.41±0.02	0.58±0.30
9.00±0.20	0.606±0.057	0.60±0.02	0.83±0.30
11.40±0.20	0.726±0.040	0.76±0.02	1.03±0.30

This result leads us to affirm that the electric field E_α and the density of rotons are closely related. To confirm this behavior we have used a pressure cell at a temperature $T = 0.937$°K and by varying the pressure in it we obtain the results shown in Fig. 7. This graph is more easily interpretable in terms of $\Delta_S - (\Delta_S)_p$, where $(\Delta_S)_p$ is Δ_S at pressure p. The difference $\Delta_S - (\Delta_S)_p$ can be compared with the equivalent difference found from neutron diffraction and by thermodynamical calculations[9,10] (Table II).

To investigate the correlation between the persistence of velocity and the extra attenuation, we have performed a series of measurements with the cell B, in the following conditions: the electric field E_{SA} is greater than E_α, the field E_{AB} is opposite in sign to the former one and is varied from zero, whereas the field E_{BC} was kept at zero The resonant cavity is placed in the area between the grid B and the collector C. A decrease of ΔT is observed when the field E_{AB} is increased from its zero value and the field E_{SA} is fixed. The decrease of ΔT continues until E_{AB} reaches a certain value E_S (stopping field) at which the extra attenuation coefficient becomes zero. An example of how the field E_S is determined is shown in Fig. 8. When measuring the

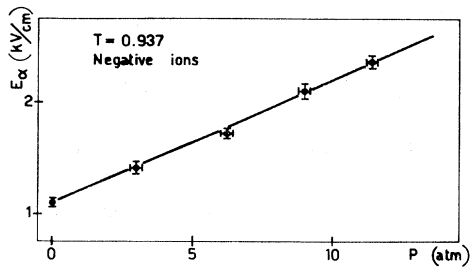

FIG. 7. The threshold field E_α is plotted, at a fixed temperature, versus the pressure.

[9] D. G. Henshaw and A. D. Woods, in *Proceedings of the Seventh International Conference on Low-Temperature Physics, 1960*, edited by G. M. Graham and A. C. Hollis (University of Toronto Press, Toronto, 1960), p. 64. D. G. Henshaw, Phys. Rev. Letters 1, 127 (1959).

[10] C. J. N. Van Den Meijdenberg, Ph.D. thesis, Leiden, 1961 (unpublished).

decrease of the amplitude variation ΔT by increasing E_{AB}, one observes at the same time the decrease of the current i_C at the collector. The behavior of i_C with respect to E_{AB} is also represented in Fig. 8. A plot of the stopping field E_S versus the extraction field E_{SA} is given in Fig. 9, for a range of temperatures: $0.878 < T < 0.985$°K. The last mentioned measurements have been made with different cells and different distances between the electrodes and have led us to conclude that the decrease of ΔT is due to the effect of an electric field and not to that of an electric potential. The dependence of E_S on E_{SA} seems to be independent of temperature in the range of temperatures of our measurements, if we exclude the part where E_{SA} is little greater than E_α. The values of the extraction field E_{SA} at zero stopping field E_S are just the E_α's.

When E_{SA} is little greater than E_α the determination of E_S is quite difficult, because one has to measure the zeroing of a very small ΔT. The possible hypothesis that, when $E_{SA} > E_\alpha$, there could exist a sort of turbulence in the whole cell, is excluded by adding to the cell in Fig. 2(b) a second resonant cavity, still orthogonal to the ionic beam direction, but behind the source with respect to the first cavity. Indeed, no extra attenuation on this second resonant cavity is observed when we are measuring a large ΔT in the first cavity.

B. Positive Ions

As far as positive ions are concerned, it has not been possible to develop a sufficiently complete scheme of measurements because of two main limitations:

(a) The variation of the amplitude of the second-sound is smaller for positive than for negative ions at the same temperature.

(b) The threshold field E_α^+ for positive ions is higher than that for negative ions E_α^- at a fixed temperature.

In any case it is possible to draw the following conclusions:

(1) The field E_α^+ coincides with the field of the minimum of the drift velocity E_M^+.

(2) The field E_S^+ which stops the ionic current zeroing the second-sound amplitude variation ΔT is smaller than E_S^-.

(3) The penetration depth which is connected to the "persistence" of velocity is for positive ions about one fifth of the corresponding penetration depth of negative ions with the condition $E_{SA}^+/E_\alpha^+ = E_{SA}^-/E_\alpha^-$.

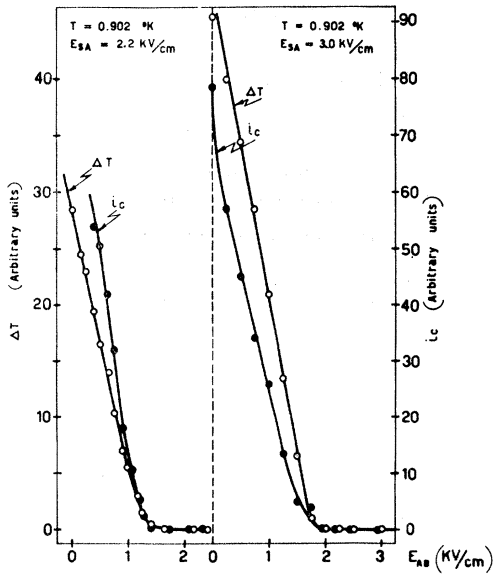

FIG. 8. Decrease of the amplitude variation ΔT and collector current i_C with increasing the field E_{AB} opposite to the constant extraction field E_{SA}. The zeroing of ΔT corresponds to the stopping field E_S.

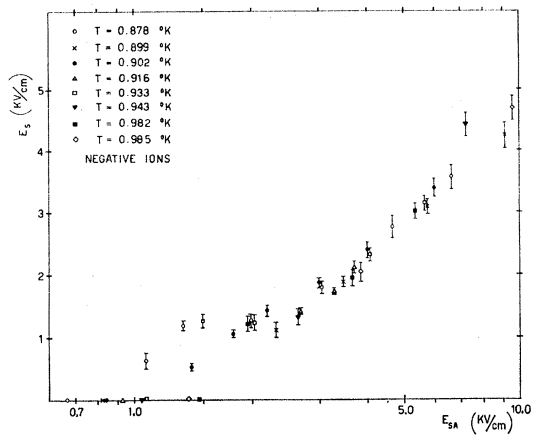

FIG. 9. The stopping field E_S is plotted versus the extraction field E_{SA} on a logarithmic scale. The values of E_{SA} at zero stopping field are just the threshold field E_α's. Different symbols refer to the different temperatures listed. The error for E_S is due mainly to the uncertainty in the graphical method of determining it.

DISCUSSION

We want to discuss here the results given in the preceding section (from a general point of view) and draw some conclusions on the physical features of the phenomenon, without any reference to a particular model.

(1) The sharp decrease which appears in the drift velocity of the ions has been explained previously in terms of a simple model, implying the existence of a vortex ring closely bound to the ions. This model gives values in good agreement with the experimental data until the field E_M is reached. However, the extra attenuation which arises at the minimum can not be explained with the Huang and Olinto model,[11] which states that the vortex ring, even for fields $E > E_M$, continues increasing its radius and that thereafter the measurements of the drift velocity are influenced by the boundary conditions.

Indeed, by assuming a friction force between normal and superfluid proportional to the length of the vortex

[11] K. Huang and A. C. Olinto, Phys. Rev. 139, A1441 (1965).

lines such as the force used by Hall and Vinen,[4,5] one gets an extra attenuation coefficient proportional to the length of the vortex lines.

The relation between the velocity and the radius of a vortex ring is

$$v=\frac{K}{4\pi r}\left(\ln\frac{8r}{a_0}-\frac{1}{4}\right), \tag{5}$$

where $k=nh/m$ is the circulation, h=Planck's constant, m=He atom mass, $n=1, 2, 3, \cdots$, a_0=radius of the core, and r=radius of the vortex ring.

By using the relation (1), which is equivalent to the result obtained by Huang and Olinto, one can find an exponential dependence of the vortex length and the extra attenuation coefficient upon the electric field. This is in clear contradiction with our experimental data, which exhibit a linear dependence of the extra attenuation coefficient upon the electric field.

Moreover an explanation in terms of (1) and (5) does not explain the high value of the extra attenuation coefficient we measure. In fact the extra attenuation we find is of the same order of magnitude as that found by Hall and Vinen and Peshkov.[4,5]

However, the power dissipated by our electric field is less than 10^{-7} W/cm^2 compared with 10^{-2} W/cm^2 of the Vinen and Peshkov experiments. In order to explain the extra attenuation we observe in terms of vortex lines density, according to the attenuation coefficient found in rotating helium experiment,[4] we should have a total length of vortex lines per unit volume $10^3/10^4$ cm^{-2}. Our charge density is 10^6 ions/cm^3 so that to have the equivalent vortex lines density we would have to have at an electric field close to the minimum E_M, vortex rings of 0.1 mm radius. This value of the vortex ring radius cannot be simply explained with the model that accounts for the sharp decrease of the drift velocity[1,11] which gives $\sim$1000 Å at E_M.

(2) It is certain that the cause of the extra attenuation is an entity strictly bound to the ion. That is ions in a field $E_{SA}>E_\alpha$ cannot create a free turbulence propagating in the whole cell, which could cause the extra attenuation. The absence of free turbulence is confirmed by the following experimental facts:

(a) the lack of extra attenuation in a resonant cavity orthogonal to the ionic beam behind the source as already described;

(b) the existence of a stopping field E_S, which coincides with the field that cancels the current at the collector i_C;

(c) the direct dependence of the stopping field upon the extraction field E_{SA} shows that the ion in the field E_{SA} cannot generate a succession of vortices. This behavior would imply that the ions detach from the vortices after a time much shorter than their time of flight between the source S and the first grid A, and immediately create a new vortex. Therefore we should find a stopping field independent of the extraction field E_{SA};

(d) the linear dependence of the extra attenuation upon the charge density ρ.

(3) The extra attenuation of second-sound manifests itself as a threshold phenomenon at a field E_α corresponding about to the minimum of the drift velocity of the ions. The existence of a threshold is confirmed by the threshold behavior of the "persistence" of the drift velocity. The presence of a threshold suggests, moreover, that at the field E_α there is a change in the hydrodynamical regime, the origin and nature of which has not been yet identified.

(4) The value of E_α depends linearly on the density of the normal fluid ρn as is shown in the Table II and in Fig. 6. This behavior also corresponds to the dependence of E_C on temperature.

(5) Within the limits of the sensitivity of our method, no difference has been detected between the extra attenuation of a second-sound wave propagating parallel and perpendicular to the ionic beam. We can conclude therefore that our phenomenon is isotropic.

CONCLUSION

The extra attenuation phenomenon so far is not understandable in terms of the vortex model given for the sharp decrease of the drift velocity. It should be clarified by a proper model and theoretical treatment, which should at the same time contain an explanation of the "persistence" of the drift velocity.

ACKNOWLEDGMENT

We want to thank Professor Careri for many profitable discussions during the course of this work.